Numerical and experimental evaluation of flue gas recirculation for syngas combustion

Numerical and experimental evaluation of flue gas recirculation for syngas combustion

G Allesina, M Puglia, N Morselli, S Pedrazzi, M Parenti, F Ottani and P Tartarini

BEELab (Bio Energy Efficiency Laboratory), Department of Engineering "Enzo Ferrari", University of Modena and Reggio Emilia, Via Vivarelli 10/1 – 41125 Modena, Italy.

Corresponding author's e-mail: giulio.allesina@unimore.it

Abstract. Biomass gasification can be an interesting solution for the energy production to fight global warming and the environment pollution. The flare apparatus is an essential component of gasification systems, but considering small scale ones, it is often quite simple and not very optimized. A way to minimize the NOx production during the combustion is recirculating the flue gas into the flames, making the combustion zone cold and inhibiting the nitrogen oxides formation. In this work different flare designs were numerically evaluated through OpenFOAM software to find the best flare shape that can guarantee the flue gas recirculation. Simulations results were verified building and testing a flare with an optimized geometry for a small-scale gasification system. Numerical simulation and experimental tests shown that it can be possible to design a simple flare for syngas combustion that guarantee low combustion temperature through flue gas recirculation.

1. Introduction

Gasification is a very promising way to produce energy through renewable sources like wood wastes and agricultural residues [1]. Through this process, a gaseous fuel known as syngas is produced [2]. Syngas is composed of a mixture of H_2, CO, CO_2, CH_4, H_2O and N_2 [3] and it can be used in Internal Combustion (IC) engines for energy production [3]. However, syngas can also be burnt in a flare to produce heat with emissions lower than to biomass combustion.
The design of small-scale gasification systems flares is often quite simple and not really optimized for a clean combustion, in fact they are used only during the start-up of the gasifier. Considering that nitrogen oxides formation increases exponentially with temperature [3], flue gas recirculation can lower the emission of syngas combustion [4]. In special condition, where the flame front is avoided mixing together fuel and air with entrained recirculated combustion products, flameless combustion can be achieved [5]. This kind of combustion is very efficient and ensure very low NOx emissions [5]. The aim of this work is to find a very simple flare design that can allow flue gas recirculation that can be applied in small scale gasification systems.

First, various CFD simulations were carried out with OpenFOAM, using as a starting point the tutorial smallPoolFire2D to identify possible combustion chamber geometries to test. Once a couple of promising geometries were identified, a combustion chamber test – bench was designed and built. The syngas generated by an All Power Labs PP30 gasifier [6] was used to provide the gas. Nine K – type

thermocouples were used to measure the temperature trends inside the chamber to understand the behavior of the flame.

2. Material and methods

2.1 CFD analysis

First, a batch of CFD analyses were performed through the open source CFD toolbox OpenFOAM. The smallPoolFire2D tutorial was modified and used for the simulations. It is a 2D domain where methane is supplied through a small opening at the bottom face [7]. The boundary conditions of the top, bottom and lateral faces were patch type while front and back were empty type being a 2D simulation. The solver used was fireFOAM, it is a code developed to solve Large Eddy Simulation (LES) of fire plumes [8] through the kEqn model (one equation Eddy-Viscosity model [9]). The fuel of the combustion simulation was methane, that is just one of the various components of syngas. However, it was chosen to not vary the gas composition in this first study.

2.1.1 First geometry

The first combustion chamber geometry tested was the tutorial domain as it is, varying only the CH_4 inlet velocity, inlet dimension, the dimension of the domain and the number of cells of the mesh. Considering that the volume flow of the flue gas produced with methane combustion is about 6.1 times higher compared to the syngas one, it was assumed that the methane volume flow should be 6.1 lower compared to the syngas one. It is important to underline that the interest is on the behavior of the flames rather than the energy comparison between the two fuels. A possible syngas flow during the start-up phase can be 3.8 m^3/h, and considering an inlet dimension with a 5 cm diameter, the syngas velocity would be 0.53 m/s, therefore the methane velocity was set to 0.087 m/s. As said before, the inlet dimension was set to 5 cm to represent the 1 ½ inches pipe used in the experimental test. The dimensions of the domain were set to 30 cm base and 30 cm height, in order to have something compact and easy to build for the experimental tests. This first simulation was carried out to compare this domain, with only minor modifications, to other geometries that aim to recirculation. Three different mesh subdivisions with 2500, 10000 and 40000 cells (**Figure 1**) were tested to investigate the mesh sensitivity.

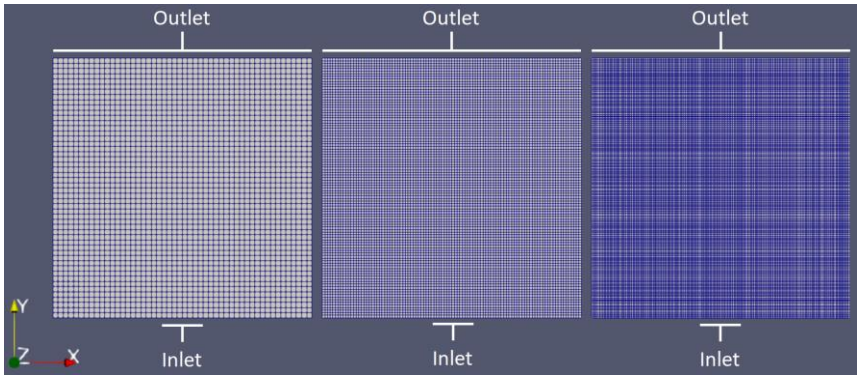

Figure1. 1st geometry tested with three different mesh generations

The temperature trend was evaluated considering 9 cells of the mesh and the maximum temperature of the domain. The position of these cells was the same for all the simulations performed in this work. In **Figure 2** it is possible to see their position and how they were labelled.

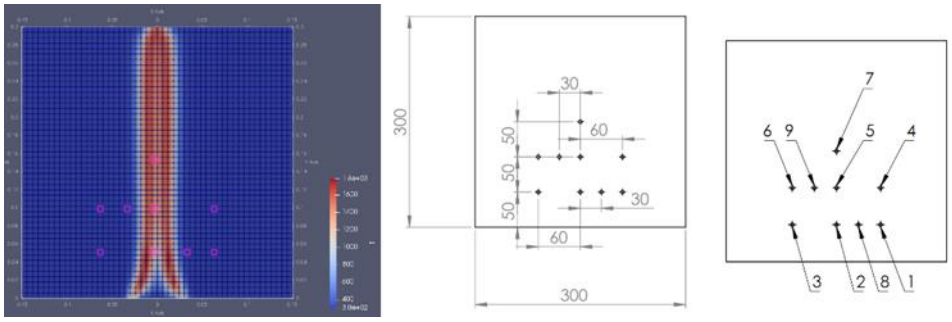

Figure 2. Cells position and labelling for temperature trend

The time of the simulation was set for 5 seconds and the residues were logged. In particular, the residues of the velocity in the x and y direction (U_x and U_y) and the heat transfer coefficient one (h).

2.1.2 Second and third geometry

The aim of second and third geometry simulated was to promote the flue gas recirculation. The modification for the second geometry was the addition of wall type faces in the upper part of the domain and in the two sides (**Figure 3**). Even for this geometry three mesh subdivisions were tested, with 1584, 6336 and 25344 cells respectively.

Unlike the second one, for the third geometry the upper wall added in the domain was not flat but curved, and there were two outlets instead of one (**Figure 3**). Three mesh subdivision were tested with 1680, 6720 and 26880 cells.

The temperatures were evaluated in the same position of the first geometry as well as the maximum temperature of the domain. Even in these case the same residues were logged.

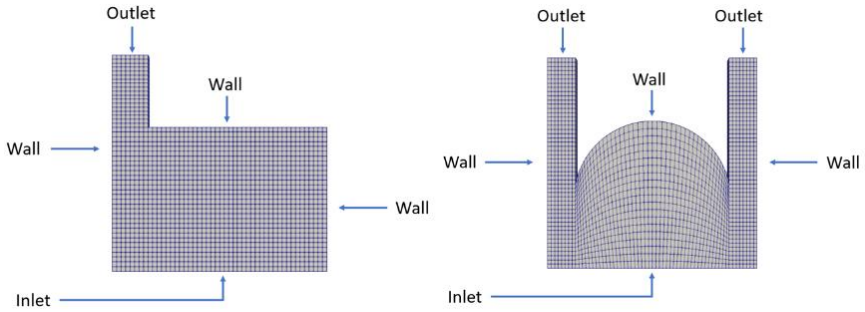

Figure 3. 2nd (left) and 3rd (right) geometries

2.2 Combustion chamber design

Once obtained the first promising results from the CFD analysis, a combustion chamber was design and built. The aim was to design something that can be easily changed in order to test different geometries. A box-shaped chamber was built in mild steel sheet, except for the front that was made in ceramic glass to visually inspect the flame behaviour during the tests. The housing for 16 thermocouples was prepared and 9 K – type ones were positioned in the same position of the cells considered in the simulations, half a way between the front and the rear of the chamber. The dimensions of the combustion chamber were the same of the domain considered in the CFD simulation concerning base and height, while the depth was 23 cm (**Figure 4**).

Figure 4. Design and construction of the chamber

With other 2 metal sheets, a flat and a curved one, that can be properly connected to the chamber through 2 threaded rods, it was possible to obtain a combustion chamber very similar to the second or to the third geometry.

2.3 Experimental test

The experimental tests were carried out burning the syngas produced with the Power Pallet 30 gasifier. The gas was produced through the gasification of vine pruning pellets. A 1 ½ inches pipe was placed just below the combustion chamber to propagate the flame inside it. 9 thermocouples and 2 Pico Log Recorders were used to measure the temperature in the 9 points of the combustion chamber considered in the numerical simulations, with the highest frequency possible for the instrument, about 64 Hz. All three geometries were tested for more than ten minutes (**Figure 5**). After the tests the data have been processed and analysed

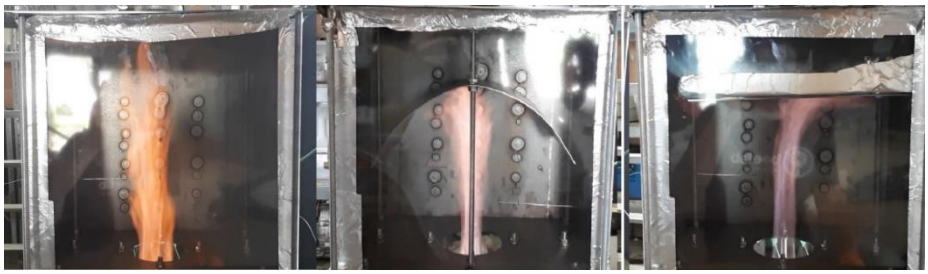

Figure 5. Syngas combustion tests in the three geometries

3. Results

3.1 CFD results - First geometry

In **Figure 6** an image of the temperature distribution in the first geometry at time 5.0 s for each mesh subdivision is shown.

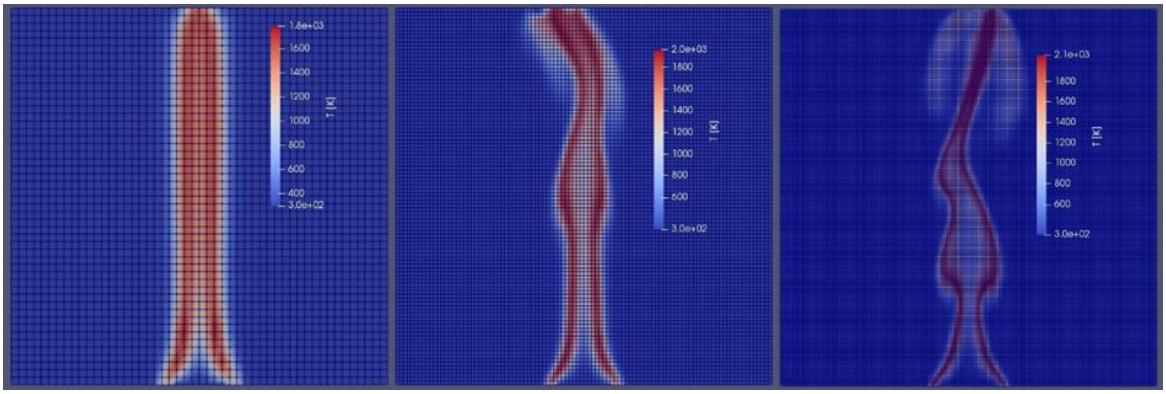

Figure 6. Temperature across the domain for 2500, 10000 and 40000 cells meshes – 1st geometry

Table 1 shows the average temperatures over time of the 9 cells considered in the meshes, the average maximum temperature over time in the domain, and the global mean temperature of the domain at time 5.0 s.

Table 1. Average temperatures in the 2500, 10000 and 40000 cells meshes – 1st geometry

Mesh [cells]	1 T [K]	2 T [K]	3 T [K]	4 T [K]	5 T [K]	6 T [K]	7 T [K]	8 T [K]	9 T [K]	Max T [K]	Global mean T 5.0 s [K]
2500	303	954	303	304	1177	304	1283	307	309	1684	448
10000	303	760	303	304	994	304	1153	305	306	1820	447
40000	303	659	303	303	925	303	1207	305	382	1910	447

It is possible to see that the maximum temperature inside the domain was higher for the domains with more cells while the global mean temperature was quite constant. In all 3 cases the temperatures in the cells 2, 5 and 7, that are the central ones (**Figure 2**), are much higher compared to the others. **Figure 7** shows the temperature trend over time inside the 40000 cells domain.

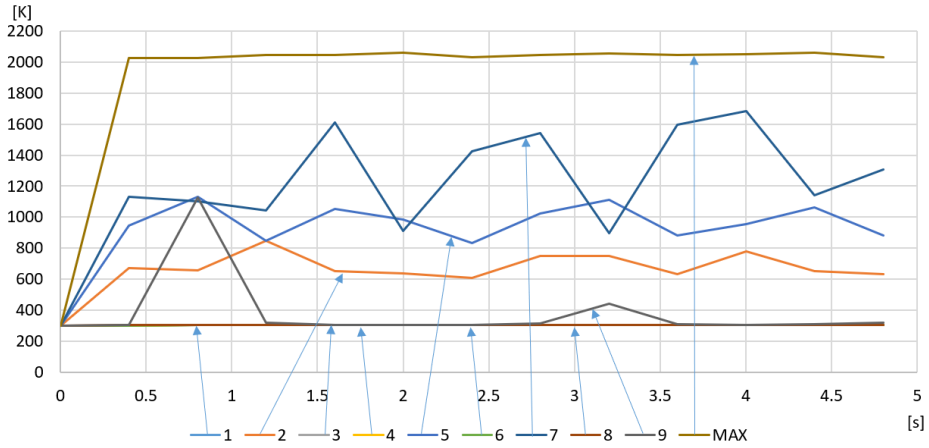

Figure 7. Temperature trend of the 40000 cells mesh – 1st geometry

The residues for all the meshes subdivisions had a decreasing trend that became stable, and they were smaller in the simulation with the highest number of cells.

3.2 CFD results – Second geometry

In **Figure 8** an image of the temperature distribution in the second geometry at time 5.0 s for each mesh subdivision is shown.

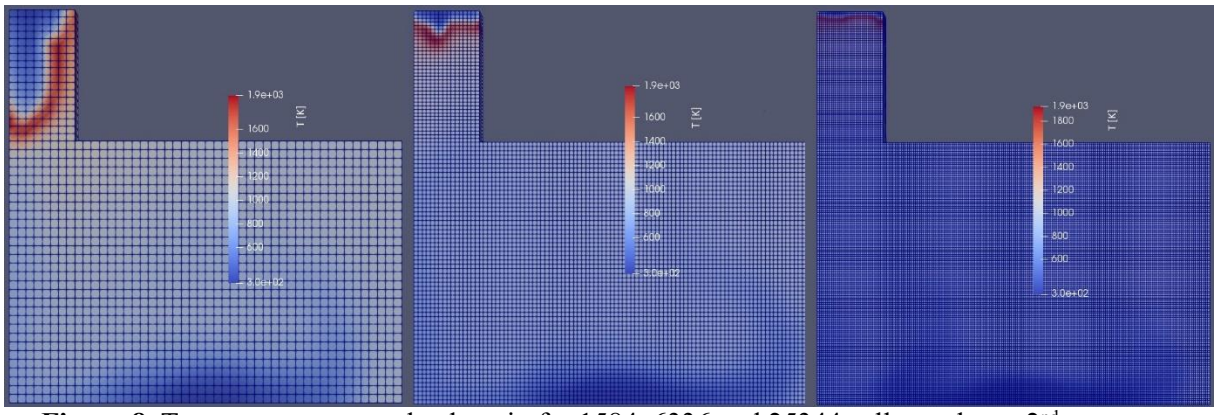

Figure 8. Temperature across the domain for 1584, 6336 and 25344 cells meshes – 2nd geometry

Table 2 shows the average temperatures over time of the 9 cells considered in the meshes, the average maximum temperature over time in the domain and the global mean temperature of the domain at time 5.0 s.

Table 2. Average temperatures in the 1584, 6336 and 25344 cells meshes – 2nd geometry

Mesh [cells]	1 T [K]	2 T [K]	3 T [K]	4 T [K]	5 T [K]	6 T [K]	7 T [K]	8 T [K]	9 T [K]	Max T [K]	Global mean T 5.0 s [K]
1584	981	911	1028	1004	955	1087	1118	960	962	1870	895
6336	887	931	1056	980	969	1061	1060	867	915	1866	830
25344	886	932	1057	998	953	960	964	860	900	1883	800

This time the temperatures in all the 9 cells considered were quite similar to one another, and this can also be seen in **Figure 9** where their trends over time is plotted for the configuration with the highest number of cells (25344). The maximum temperature was higher comparing this second geometry to the first one concerning the two meshes with less cells while in the ones with more cells it was slightly lower for this second geometry. The global mean temperature was always higher in the second geometry compared to the first one.

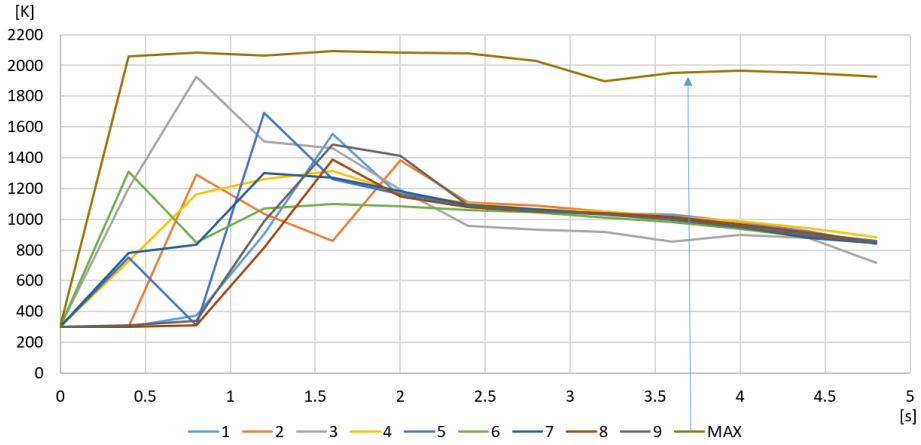

Figure 9. Temperature trend of the 25344 cells mesh – 2nd geometry

From **Figure 9** it is possible to see that the temperatures in the middle of the domain decreased with time indicating that the flame front moved away from the initial position. Considering the domain with the highest number of cells, a higher global mean temperature and a lower peak temperature can indicate a more uniform combustion, that is useful to lower the emissions [5].

Even in this case, the residues for all the three mesh subdivisions had decreasing trends that became stable after a certain number of steps, furthermore for the domain with the highest number of cells the residues became considerably smaller compared to the other two cases.

3.3 CFD results – Third geometry

In **Figure 10** an image of the temperature distribution in the third geometry at time 5.0 s for each mesh subdivision is shown.

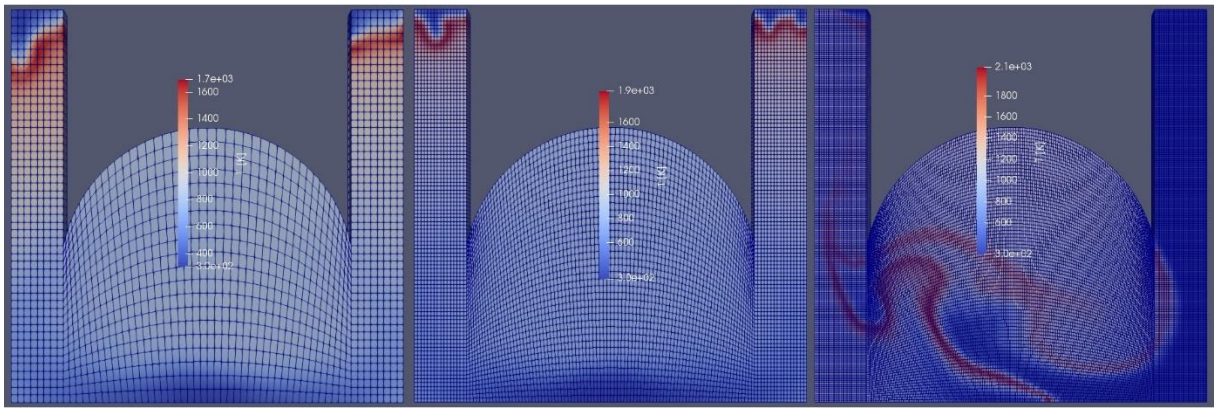

Figure 10. Temperature across the domain for 1680, 6720 and 26880 cells meshes – 3rd geometry

Table 3 shows the average temperatures over time of the 9 cells considered in the meshes, the average maximum temperature over time in the domain, and the global mean temperature of the domain at time 5.0 s.

Table 3. Average temperatures in the 1680, 6720 and 26880 cells meshes – 3rd geometry

Mesh [cells]	1 T [K]	2 T [K]	3 T [K]	4 T [K]	5 T [K]	6 T [K]	7 T [K]	8 T [K]	9 T [K]	Max T [K]	Global mean T 5.0 s [K]
1680	1037	983	1017	1039	1030	1047	1022	962	1037	1640	810
6720	964	884	958	993	1070	991	1048	1104	970	1786	824
26880	1112	1143	1102	1054	1137	1070	1153	1187	1028	1943	930

The cases with 1680 and 6720 cells were similar to the second geometry concerning the temperature trends, and from **Figure 10** it is possible to see that the flame front was near to the two outlets. For the mesh with 26880 cells the situation was more unstable, like the flame front position. Both maximum and global mean temperature increased increasing the number of cells. **Figure 11** shows the temperature trend over time inside the 26880 cells domain.

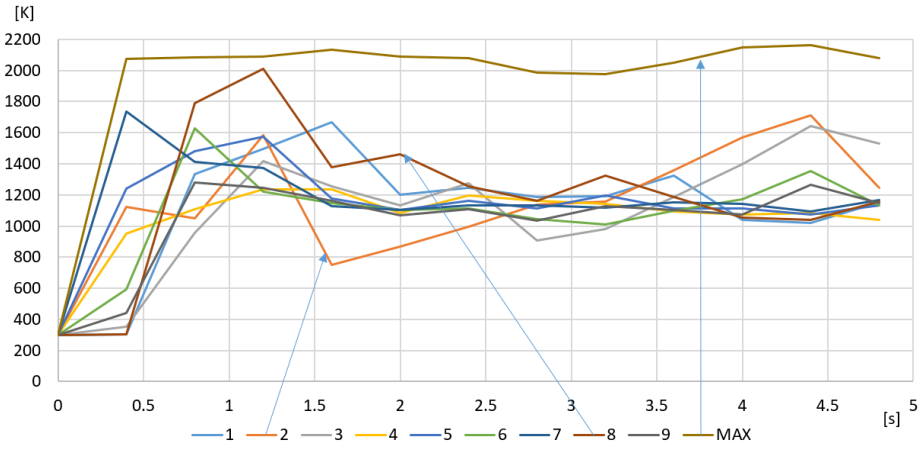

Figure 11. Temperature trend of the 26880 cells mesh – 3rd geometry

The residues for the mesh with 1680 and 6720 cells had decreasing trends especially after a certain number of steps while for the last one they increased again stabilizing on higher values, making the results obtained for this third geometry less reliable compared to the ones obtained for the first and the second one.

3.4 Experimental results – First geometry

Figure 12 shows the 9 temperature trends logged through the thermocouples (TC) positioned in the combustion chamber during the test of the first geometry configuration.

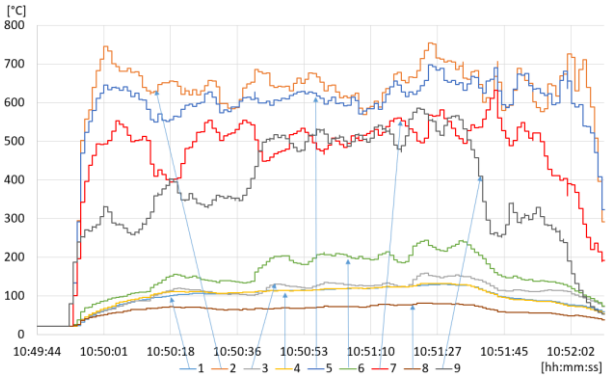

Figure 12. Temperature trends logged through the 9 thermocouples – 1st geometry

It is possible to see that the temperatures measured in the central part of the combustion chamber (TC 2, 6 and 7) were much higher than the others. In **Table 4** the average of the measured temperatures are summarized. Unlike numerical simulation, it was not possible to know neither the highest temperature reached in the domain (in this case in the combustion chamber) nor the global mean temperature. However, the average temperature logged through the 9 thermocouple can be useful to compare the various configurations.

Table 4. Average temperatures measured by the 9 thermocouples – 1st geometry

TC n°	1	2	3	4	5	6	7	8	9	Average
T [K]	381	923	392	383	891	444	783	342	691	581

3.5 Experimental results – Second geometry

Figure 13 shows the 9 temperatures logged through the thermocouples positioned in the combustion chamber during the test of the second geometry configuration. Even this time the three highest temperatures were the central ones but, unlike before, the difference between the highest and the lowest has been reduced both by the drop the highest temperatures and by the increasing of the lowest ones.

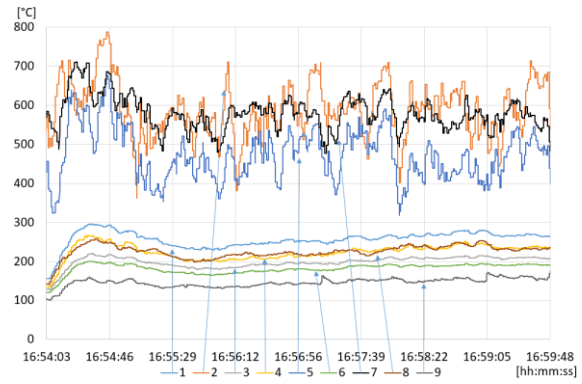

Figure 13. Temperature trend logged through the 9 thermocouples – 2nd geometry

In **Table 5** the average of the measured temperatures are summarized.

Table 5. Average temperatures measured by the 9 thermocouples – 2nd geometry

TC n°	1	2	3	4	5	6	7	8	9	Average
T [K]	523	846	467	489	738	451	844	492	416	585

Even if the temperatures measured though the thermocouples were on average higher compared to the first geometry (585 K compared to 581 K), the highest temperatures measured in the first configuration (TC n° 2 and 5 in **Table 4**) were higher than the highest ones measured in the second geometry (TC n° 2 and 4 in **Table 5**). This can be a further indication of a more uniform combustion obtained in this second geometry.

From **Table 5** it is also possible to see that the temperatures were higher on the right side (TC n° 4, 1 and 8) of the combustion chamber even if the outlet is on the left side (TC n° 9, 6 and 3).

This could indicate that the flame tended to rotate to the right as shown in **Figure 14**, then went downward to the thermocouples 4 and 8, and finally went out passing near the TC 3 and 6.

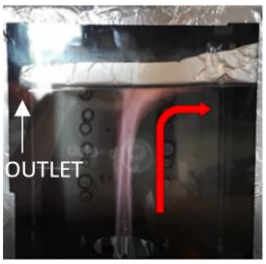

Figure 14. Combustion test in the 2nd geometry configuration

3.6 Experimental results – Third geometry

Figure 15 shows the 9 temperatures logged through the thermocouples positioned in the combustion chamber during the test of the third geometry configuration. Once again, the three highest temperatures were the central ones and, this time, the difference between the highest and the lowest temperatures is higher compared to the second geometry.

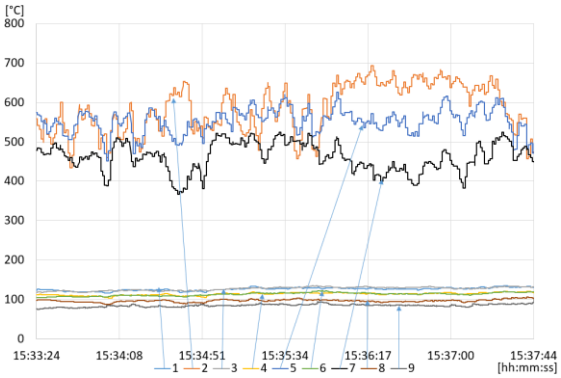

Figure 15. Temperature trends logged through the 9 thermocouples – 3rd geometry

As is possible to see from **Table 6** the average temperatures are highly symmetric considering the left and the right side of the combustion chamber (in **Figure 2** it is possible to see that the position of TC number 6 and 3 were in the opposite side of TC number 4 and 1).

Table 6. Average temperatures measured by the 9 thermocouples – 3rd geometry

TC n°	1	2	3	4	5	6	7	8	9	Average
T [K]	400	880	402	388	833	388	733	370	359	528

Considering that the central part is the hottest but after that the thermocouples that measured the higher temperatures were the 3, 1, 6 and 4, and they were further away to the centre compared to the 9 and 8 (**Figure 2**), an hypothesis is that the hot flue gas made a rotation that went around this last two thermocouples as shown in **Figure 16**.

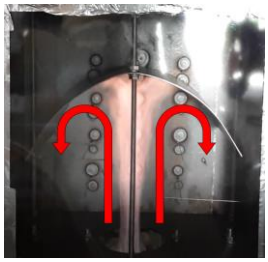

Figure 16. Combustion test in the 3rd geometry configuration

4. Conclusions

In conclusion, both CFD simulations and experimental tests has provided many clues about the possibility to make the flue gas recirculate through very simple changes in a combustion chamber like positioning a flat or a curved baffle. Especially the second geometry with the flat baffle has shown promising results in terms of temperature homogenisation, flame curvature and stability of the CFD simulation. The difference in absolute value between the measured temperatures and the calculated one was probably due to the different fuels considered (with different HHV) and the heat losses in the experimental tests. However the temperature trends of the numerical analysis and experimental tests were quite similar. A direct emission analysis of the combustion, together with the measurement of the thermal efficiency of the system can improve the understanding of flue gas recirculation phenomenon and its effectiveness, while the modelling of the combustion of syngas with the addition of heat losses can improve the numerical analysis.

References

[1] M. Puglia, N. Morselli, P. Tartarini, Design and First Tests of a Lab Scale (2KG/H) Gasifier, EUBCE Proceedings, 2019, pp. 797–801, DOI: 10.5071/27thEUBCE2019-2CV.2.12
[2] Martínez J D, Mahkamov K, Andrade R V, and Silva Lora E E, 2012, Syngas production in downdraft biomass gasifiers and its application using internal combustion engines (Renewable Energy, Issue 38) pp. 1-9 DOI: 10.1016/j.renene.2011.07.035
[3] Mason, J., Kaufmann, B., Tartarini, P., Puglia, M., Morselli, N., Veratti, G., Bigi, A, Compression Ratios Comparisons between Engines Operating with Producer Gas, EUBCE Proceedings, 2019, pp 1927–1931, DOI: 10.5071/27thEUBCE2019-IBV.1.8
[4] Ismo Roiha, Juha Kaikko, Keijo Jaanu, Esa Vakkilainen, Analysis of high flue gas recirculation for small energy conversion systems, Applied Thermal Engineering, Vol 63, pag 2018-226. 2014, DOI: 10.1016/j.applthermaleng.2013.10.062
[5] Milani A., Wünning J.G. (2007) Flameless Oxidation Technology. In: Syred N., Khalatov A. (eds) Advanced Combustion and Aerothermal Technologies. NATO Science for Peace and Security Series C: Environmental Security. Springer, Dordrecht, DOI: 10.1007/978-1-4020-6515-6_26
[6] July 2020 available: http://www.allpowerlabs.com/pp30-power-pallet website
[7] July 2020 available: http://www.cfdyna.com/Home/OF_Combustion.html website
[8] Y. Wang, P. Chatterjee, J. L.de Ris, Large eddy simulation of fire plumes, Proceedings of the Combustion Institute, Vol. 33, Issue 2, 2011, pp. 2473–2480, DOI: 10.1016/j.proci.2010.07.031
[9] OpenFOAM The Open Source CFD Toolbox User Guide, Version v1712, 4th January 2018, OpenCFD Limited